2009 American Control Conference
Hyatt Regency Riverfront, St. Louis, MO, USA
June 10-12, 2009

An Iterative Algorithm for Model-Based Predictive Control of an Electro-Pneumatic Valve Actuator

Guoming G. Zhu, Jia Ma, and Harold Schock

Abstract: The benefits of utilizing camless valve actuations for internal combustion engines are primarily due to their ability of significantly improving engine performance. There are mainly three kinds of camless valve actuators: electro-magnetic, electro-hydraulic, and electro-pneumatic valves. This paper focuses on controls of the Electro-Pneumatic Valve Actuators (EPVA). The model-based predictive control scheme has been developed for exhaust electro-pneumatic valve actuators to overcome variable in-cylinder pressure force as a function of engine operational conditions in early publications. But high computational throughput of predictive control makes it extremely difficult for real-time implementation. This paper develops an iterative model-based predictive control scheme for lift control of an exhaust EPVA that significantly reduces computational throughput. The developed iterative control strategy was verified in simulation using an EPVA model that combines mathematical models of exhaust valve and in-cylinder pressure based upon a 5.4 Liter 3 valve V8 engine head.

I. INTRODUCTION

Variable intake valve timing and lift can be used to optimize engine performance over a wide operating range, for instance, to reduce engine pumping losses, deactivate selected cylinder(s), and control flame speed by manipulating in-cylinder turbulence. Exhaust valve timing and lift control makes it possible to vary the amount of Residual Gas Recirculation (RGR) and control valve overlap when combined with intake valve control. Variable valve timing and lift control are also a key technology for Homogenous Charge Compression Ignition (HCCI) combustion control.

Variable valve actuation can be achieved with mechanical (cam-based), electro-magnetic (electric mechanical), electro-hydraulic, and electro-pneumatic valvetrain mechanisms. The cam based variable valve actuation is able to provide either a multiple stepping or a continuously changing valve timing phase shift. See [1], [2] and [3]. Infinitely variable valvetrain, often referred as camless valvetrain, includes electro-magnetic ([4], [5], [6], [7], and [8]), electro-hydraulic ([9], [10], and [11]), and electro-pneumatic actuations ([12] and [17]}. The electro-pneumatic valve actuator (EPVA) utilizes the supplied air pressure to actuate either the intake or exhaust valve by electronically controlling two solenoids that regulate the motion of the actuator's piston. For both electro-hydraulic and electro-pneumatic valves, there is a potential issue of having a repeatable valve lift over the life of an engine.

Valve lift control for camless valvetrain actuation has been investigated by a number of researchers. Adaptive peak lift control was presented in [15], and digital valve technology was applied to control of a hydraulic valve actuator in [16]. The modeling and control for electro-mechanical valve actuator is discussed in [8], and modeling and control of electro-pneumatic valve actuators were shown in [12], [13], [14], and [17].

Unlike the intake valve, the engine exhaust valve opens against an in-cylinder pressure that varies as a function of the engine operational conditions with cycle-to-cycle combustion variations. This pressure disturbance force slows down the valve actuator response and as a result, it increases the variation of valve opening delay. In fact, this disturbance makes it difficult to maintain repeatable valve opening timing and lift over engine operational range. A model-based predictive EPVA lift control algorithm was presented in [17]. This controller consists of two parts: feedforward and closed loop controls. The predictive control is used to provide a feedforward lift control based upon the predicted valve lift, while the closed loop controller is used to minimize the mean control error. This paper presents an iterative predictive control strategy to reduce online microprocessor throughput. The developed strategy was verified in simulation using the combined mathematical models of exhaust valve and in-cylinder pressure.

The paper is organized as follows. In Section II we review the predictive control of the electro-pneumatic valve actuator. Section III proposes an iterative algorithm that uses significantly less microprocessor throughput and is implementable for real-time control. The simulation validation of proposed iterative algorithm is discussed in Section IV. Section VI adds some conclusions.

II. EPVA model review and its predictive control

A physics-based EPVA nonlinear model, called a level-one model, was built component-by-component based upon the flow and fluid dynamics in [12]. This model provides an

Manuscript received August 25, 2008.

G. Zhu and H. Schock are with Mechanical Engineering of Michigan State University, 2555 Engineering Building, East Lansing, MI 48824, USA (e-mail: zhug@msu.edu for Zhu and schock@msu.edu for Schock).

J. Ma is with Delphi Corporation (e-mail: jia.ma@delphi.com).

insight to the operation of the pneumatic and hydraulic mechanical actuation system. A piecewise linearized level-two model was then created based on the level-one model to reduce the computational throughput for control system development purposes. See [13] and [17]. Level-two model was used as the actuator model for both intake and exhaust valve control designs in the previous studies.

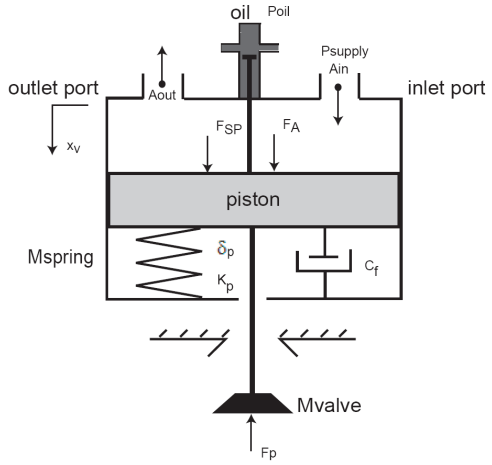

Figure 1: EPVA piston model

Figure 1 shows the schematic diagram of an EPVA. During the valve opening stage, the valve actuator can be modeled as a second order mass-spring-damper system with zero initial conditions. See Equation (2.1).

$$M\ddot{x}_V + C_f \dot{x}_V + K_p x_V = F_A - F_P - F_{SP}, \qquad (2.1)$$

where, M is the equivalent mass [17] of actuator piston, effective valve spring mass, exhaust valve and cap; C_f is the damping ratio approximating energy dissipation due to flow loss and frictional loss; K_P is the stiffness of the valve spring, respectively. On the right side of equation (2.1), F_{SP} is the constant spring preload force; F_P is the in-cylinder pressure force applied on the back of the exhaust valve; and F_A is the actuator force due to the air pressure.

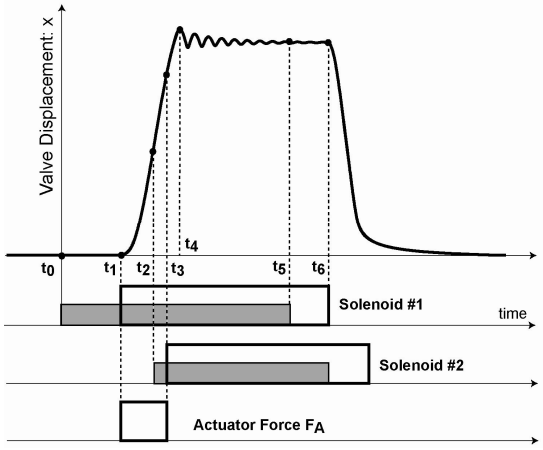

Figure 2: EPVA control scheme

Figure 2 illustrates the relationship between the solenoid control commands and the exhaust valve lift response. The valve response can be divided into three stages. They are the opening stage between t_0 and t_4, dwell stage between t_4 and t_6, and closing stage after t_6. For valve lift control, we are going to concentrate on the opening stage between t_0 and t_4.

During the opening stage, solenoid *#1* is activated at time t_0 to open the air supply valve (see Figure 1), which induces a high air pressure force F_A at time t_1 to push the valve open. The time difference between t_0 and t_1 is due to the electro-magnetic delay of solenoid *#1*. Solenoid *#2* is then activated at time t_2 to close the air supply valve and open air outlet valve, which removes the air pressure force F_A at time t_3. Again, the time difference between t_2 and t_3 is due to the electro-magnetic delay of solenoid *#2*. Note that the interplay between two solenoids results in a pulse force F_A to the actuator between t_1 and t_3. The increment of the pulse width $t_3 - t_1$ increases valve lift. With the air pressure force F_A removed, the valve movement continues until it reaches its peak lift at time t_4 (the valve equilibrium). This ends the open stage.

Next, the valve enters the dwell stage between t_4 and t_6, where it is held open by a hydraulic latch mechanism (see Figure 1). At the end of the dwell stage, solenoid *#1* is deactivated at time t_5, resulting the release of the hydraulic latch and the valve starts returning at time t_6. The time difference between t_5 and t_6 is due to the electro-magnetic delay of solenoid *#1*. The close stage starts at time t_6 (free return) and the hydraulic latch activated at the end of closing stage to have a soft landing of exhaust valve [12].

The key for exhaust valve lift control is to determine when to activate solenoid *#2* during exhaust valve opening stage for each engine cycle with the varying in-cylinder pressure force applied at the face of the exhaust valve with activation delay $t_3 - t_2$. In [17], a model-based predictive lift control algorithm is developed for exhaust valve lift control (see Figure 3). After the solenoid *#1* is activated, the predictive control scheme uses a Kalman filter to estimate both displacement x_V and velocity $\dot{x}_V$; then these estimated valves are used as inputs to predict the maximum displacement x_{MAX} assuming that solenoid *#2* was activated at this moment. If the estimated maximum displacement x_{MAX} is greater than the desired reference displacement x_{REF}, solenoid #2 is activated; otherwise, the control scheme is looped back to start a new iteration until x_{MAX} is

greater than x_{REF}. Detailed description of the predictive valve lift control can be found in [17].

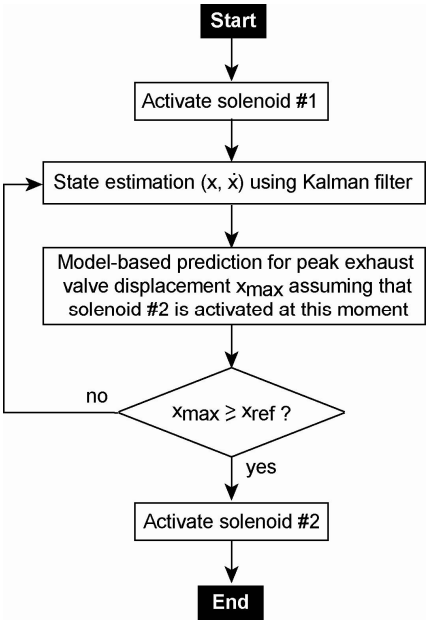

Figure 3: Feed forward exhaust valve lift control scheme

The disadvantage of this predictive control scheme in [17] is the high throughput calculation of analytic solution x_{MAX}, which makes it difficult to be implemented in a real-time control environment. The proposed iterative model-based predictive control scheme in this paper is aimed to reduce the predictive calculation throughput.

III. An Iterative Algorithm

Consider the state space realization of system (2.1):

$$\dot{x} = A_C x + B_C u, \quad u = F_A - F_P - F_{SP}, \tag{3.1}$$

where

$$A_C = \begin{bmatrix} 0 & 1 \\ -K_P/M & -C_f/M \end{bmatrix}, \; B_C = \begin{bmatrix} 0 \\ 1/M \end{bmatrix}, x = \begin{bmatrix} x_V \\ \dot{x}_V \end{bmatrix}. \tag{3.2}$$

For a given sample period *T*, the continuous system (3.1) can be discretized into the following realization:

$$x(k+1) = Ax(k) + Bu(k), \tag{3.3}$$

where *x* is a two dimensional vector with the first entry as the valve displacement x_V and the second as the valve velocity $\dot{x}_V$; and *u*(*k*) is the sum of the external forces applied to the valve.

$$u(k) = u_A(k) + u_P(k) + u_{SP}(k) \tag{3.4}$$

where $u_A(k) = F_A$ is the force due to EPVA actuation force; $u_P(k) = -F_P$ is the force applied to the valve surface due to in-cylinder pressure; and $u_{SP}(k) = -F_{SP}$ is the force due to valve spring preload force. Note that u_{SP} is a constant negative force and u_A is a pulse force; see Figure 2, with a known duration $t_3 - t_2$ whose magnitude is a function of the supply air pressure for the EPVA, assuming that $k = 0$ at time t_2. That is

$$u_A(k) = \begin{cases} F_A(P_S), & k < n, \; n = (t_3 - t_2)/T \\ 0, & k \geq n \end{cases} \tag{3.5}$$

Note that the solution of state space equation (3.1) can be written as follows:

$$x(k) = A^k x_0 + \sum_{i=0}^{k-1} A^{k-1-i} B u(i) \tag{3.6}$$

and that the above equation can be expanded as follows:

$$\begin{aligned} x(k) = {} & A^k x_0 + \sum_{i=0}^{k-1} A^{k-1-i} B u_P(i) \\ & + \sum_{i=0}^{k-1} A^{k-1-i} B u_{SP}(i) + \sum_{i=0}^{k-1} A^{k-1-i} B u_A(i) \end{aligned} \tag{3.7}$$

For a given *k*, both

$$x_{SP}(k) = \sum_{i=0}^{k-1} A^{k-1-i} B u_{SP}(i) = -F_{SP} \sum_{i=0}^{k-1} A^{k-1-i} B \tag{3.8}$$

and

$$x_A(k) = \sum_{i=0}^{k-1} A^{k-1-i} B u_A(i) = \begin{cases} F_A \sum_{i=0}^{k-1} A^{k-1-i} B, & k < n \\ F_A A^{k-n} \sum_{i=0}^{n-1} A^{n-1-i} B, & k \geq n \end{cases} \tag{3.9}$$

are independent of in-cylinder pressure after t_1 and they can be pre-calculated. Let

$$x_P(k) = \sum_{i=0}^{k-1} A^{k-1-i} B u_P(i), \tag{3.10}$$

then, equation (3.7) can be rewritten as follows:

$$x(k) = A^k x_0 + x_A(k) + x_P(k) + x_{SP}(k). \tag{3.11}$$

Define an integer index $m = 0, 1, \cdots$ as the step for updating predictive output such that

$$m = (t_2 - t_1)/T \geq 0.$$

Note that $m = 0$ represents the time at t_1, where the iterative predictive calculation starts, and let $u_m(k)$ be a discrete sequence that satisfies

$$u_m(k) = u_0(k+m) = u_{m-1}(k+1),$$

where *k* is the number of steps from *m*. Since u_A and u_{SP} are independent of *m*, equation (3.4) becomes

$$u_m(k) = u_{P\_m}(k) + u_A(k) + u_{SP}(k),$$

where

$$u_{P\_m}(k) = u_{P\_0}(k+m) = u_P(k+m) = u_{P\_m-1}(k+1).$$

Note that $u_P(0)$ is the pressure force when the calculation started (i.e., m = 0). Now, we can write the response as function of index m

$$x_m(k) = A^k x_{m\_0} + x_A(k) + x_{P\_m}(k) + x_{SP}(k), \quad (3.12)$$

where x_{m_0} is the state initial condition vector that is m steps from the t_1; $x_A(k)$ and $x_{SP}(k)$ are independent of index m; and x_{P_m} is defined as follows:

$$x_{P\_m}(k) = \sum_{i=0}^{k-1} A^{k-1-i} B u_{P\_m}(i) = A \sum_{i=0}^{k-1} A^{k-2-i} B u_{P\_m}(i).$$

Note that

$$\begin{aligned} x_{P\_m-1}(k) &= \sum_{i=0}^{k-1} A^{k-1-i} B u_{P\_m-1}(i) \\ &= \sum_{i=0}^{k-2} A^{k-2-i} B u_{P\_m-1}(i+1) + A^{k-1} B u_{P\_m-1}(0). \end{aligned}$$

Using the fact that $u_{P\_m}(k) = u_{P\_m-1}(k+1)$, we have

$$x_{P\_m}(k) = A\left\{x_{P\_m-1}(k) - A^{k-1} B u_{P\_m-1}(0)\right\} + B u_{P\_m-1}(k). \quad (3.13)$$

Equation (3.13) indicates that we can calculate state $x_{p\_m}(k)$ iteratively, so does $x_m(k)$.

Figure 4 shows a diagram of the proposed iterative algorithm, where the algorithm is executed every data sample period *T*. The algorithm can be summarized as follows:

Step 1: If solenoid *#1* is not activated, set *m = 0* and *n = 0*. Go to Step 5.

Step 2: If solenoid *#1* is activated and *n = 0*, calculate peak displacement assuming that solenoid *#2* is activated immediately after the valve starts moving,

$$x_0(k) = x_A(k) + x_{P\_0}(k) + x_{SP}(k). \quad (3.14)$$

To find the peak, the absolute value of $x_{0\_2}(k)$ is minimized, where $x_0(k) = [x_{0\_1}(k), x_{0\_2}(k)]^T$. To reduce the throughput in one sample period, this calculation is completed within a few sample periods. If the maximum is found, set $n = 1$ and $l = 0$. Go to Step 5.

Step 3: If solenoid *#1* is activated and *n* = 1, a state estimator is used to estimate current state $x_{m\_0} = [x_{m\_0\_1}, x_{m\_0\_2}]^T$ using measured x_V.

Step 4: If $x_{m\_0\_1} > x_{m\_0\_th}$ (given threshold), estimate the peak displacement, assuming solenoid #2 is activated at this sample period:

a. Calculate $x_{P\_m}(k)$ using equation (3.13) and

$$x_m(k) = A^k x_{m\_0} + x_A(k) + x_{P\_m}(k) + x_{SP}(k). \quad (3.15)$$

If $l = 0$, $h_1 = x_{m\_2}(k)$ ($x_m(k) = [x_{m\_1}(k), x_{m\_2}(k)]^T$).

b. Let $h_2 = x_{m\_2}(k)$.

If $h_1 h_2 > 0$ and $h_2 < 0$, let $l = l + 1$ and update $x_m(k-1)$ using the following equations:

$$\begin{aligned} &x_A(k-1) = A^{-1} x_A(k), \\ &x_{SP}(k-1) = x_{SP}(k) - A^{k-1} B F_{SP}, \\ &x_{P\_m}(k-1) = A^{-1}[x_{P\_m}(k) - B u_{P\_m}(k-1)]. \end{aligned} \quad (3.16)$$

Let $h_1 = h_2$ and $k = k - 1$; go to Step 4, a).

If $h_1 h_2 > 0$ and $h_2 > 0$, let $l = l + 1$ and update $x_m(k+1)$ using the following equations:

$$\begin{aligned} &x_A(k+1) = A x_A(k), \\ &x_{SP}(k+1) = x_{SP}(k) + A^k B F_{SP}, \\ &x_{P\_m}(k+1) = A x_{P\_m}(k) + B u_{P\_m}(k) \end{aligned} \quad (3.17)$$

Let $h_1 = h_2$ and $k = k + 1$; go to Step 4, a).

If $h_1 h_2 \le 0$ and $x_{m\_1}(k) \ge x_{REF}$ (desired displacement), activate solenoid #2 and complete calculation for this cycle. Otherwise, $m = m + 1$.

Step 5: Complete calculation for this sample period.

The main feature of this iterative algorithm is to use the predictive results from the last sample as initial conditions to start the search close to the peak displacement. Figure 4 shows the iterative algorithm in a block diagram.

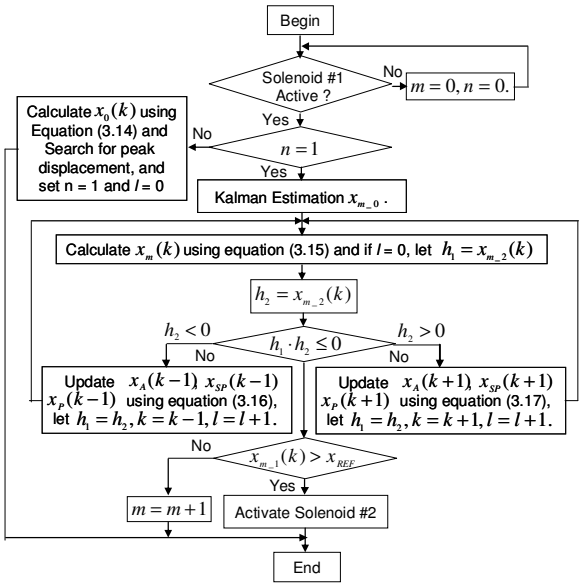

Figure 4: Iterative algorithm diagram

IV. Simulation Results

A simulation environment is developed to validate the

proposed iterative predictive control algorithm, where the level-two EPVA model, developed in [17], is used as system plant model. In order to simulate the actual engine cycle-to-cycle variation of the in-cylinder pressure, 300 cycles of the in-cylinder pressure data was collected from a 5.4 liter 3 valve V8 engine with a regular cam shaft. The pressure sensor data was used as initial condition at exhaust valve opening to simulate the in-cylinder pressure with an EPVA actuator, see [17], which was used for the validation simulation.

The closed loop control architecture is shown in Figure 5, where the control signal for valve solenoid #2 consists of feedforward predictive control and closed loop Proportional and Integral (PI) control. Note that predictive control is updated at valve control sample period (T=40μs) and the closed loop PI control is updated every engine cycle. The closed loop control feedback signal is the valve position sensor, where 5% measurement white noise is added for the simulation.

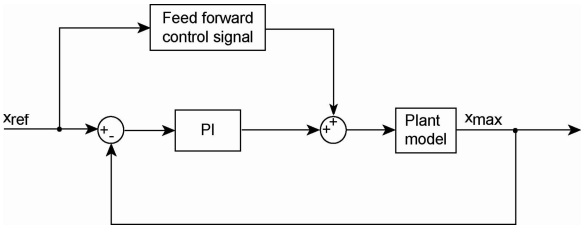

Figure 5: Closed loop control scheme

A Simulink "S" function was developed for the iterative predictive control algorithm shown in Figure 4. This "S" function is executed every 40μs. The actuator parameters used for the simulation are shown in Table 1.

Table 1: Predictive control parameters

Equivalent mass (M)	0.0734 Kg
Damping coefficient (C_f)	0.130 N-second/mm
Spring stiffness (K)	26 N/mm
Spring preload force (F_{SP})	112 N
Actuator force (F_A)	831.8 N

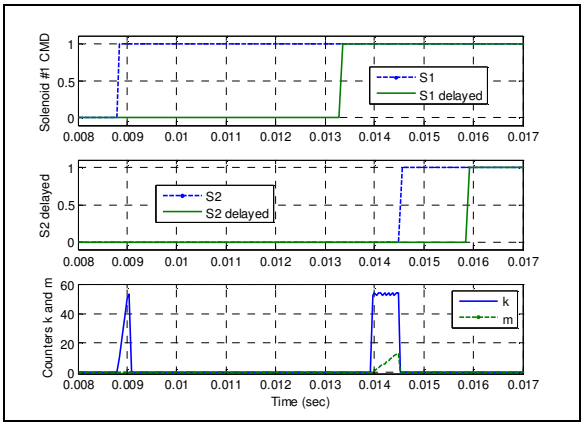

Figure 6: Iterative control event

Figure 6 shows algorithm events within one valve opening cycle. The dotted line on the top of the plot shows that solenoid #1 is activated at around 0.0088 second, and the supply pressure inlet valve (see Figure 1) is not opened until the rising edge of the solid line on the top graph due to electric-magnetic delay. The solenoid #2 is activated at around 0.0145 second (dotted line on the mid graph), which leads to closing the inlet valve and opening the outlet valve (see solid line in the mid graph of Figure 1) around 0.0158 second. The solid line in the bottom graph shows counters k and m, it can be found that after solenoid #1 is activated, it takes a few samples to complete calculating $x_0(k)$ since k increases from 0 to about 52. When the valve displacement is greater than $x_{m\_0\_th}$ (0.3 mm), the predictive algorithm becomes activate, which can be observed from the dotted line in the bottom graph (counter m increases from 0 to 14).

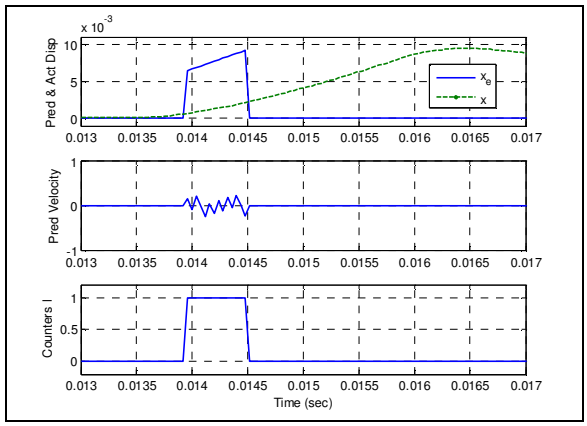

Figure 7: Iterative estimated and actual displacement

Figure 7 shows the details of the iterative prediction process, where the top graph shows both estimated and actual displacement at around 9 mm. The mid graph shows the estimated velocity that oscillates around zero to achieve maximum displacement. The bottom graph shows that for the predictive calculation, only one iteration is used to find peak displacement due to the fact that the predictive results from the last iteration are used as the initial conditions.

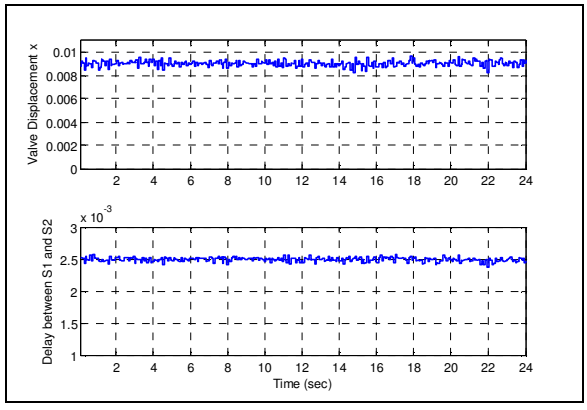

Figure 8: Steady state displacement

Figure 8 shows the steady state valve lift response of the simulation, where the reference displacement $x_{REF} = 9\,\text{mm}$ (see top graph); and the time between inlet valve opening to outlet valve opening is about 2.5 ms, see the bottom graph. It can be calculated that the mean displacement is at 9 ± 0.7 mm.

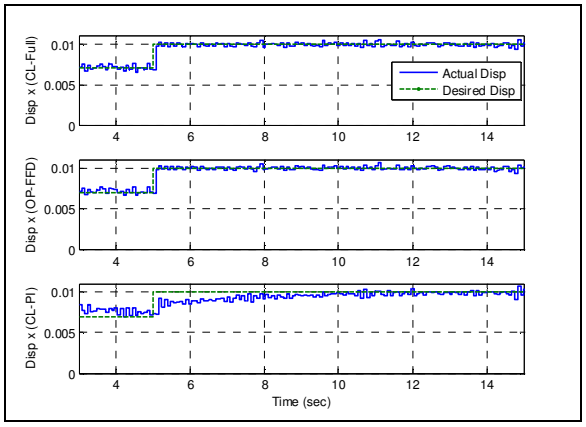

Figure 9: Step displacement responses from 7mm to 10mm

Figure 9 shows step responses of three cases from 7mm to 10 mm. For the top graph (case a), both feedforward and closed loop control are used; for the mid graph (case b) only predictive feedforward control is used; and for the bottom one (case c), only PI control is used. It can be see that for both cases a) and b), the one step transient response can be achieved, while for case c) it takes a few seconds to get to steady state. This demonstrated the importance of using the predictive control to achieve one step transient response (one of the key requirements for engine control).

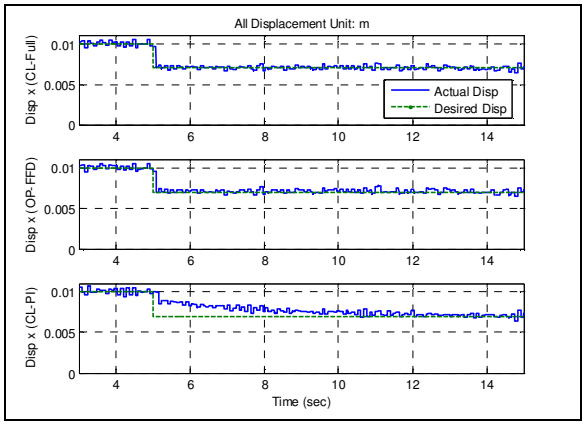

Figure 10: Step displacement responses from 10mm to 7mm

Figure 10 shows the step responses from 10 mm to 7 mm of the same three cases as what presented in Figure 9. One can conclude that the predictive control is very important for achieving one step transient response. Since only one iteration is need to find the maximum displacement, it only needs 24 multiplications to complete the predictive calculation for each sample period.

V. Conclusion

An iterative model-based predictive control strategy was developed for the feedforward control of an electro-pneumatic valve actuator. This strategy contains two main portions: state estimation of both displacement and velocity based upon the displacement feedback and iterative model-based displacement prediction. The developed feedforward control, combined with the closed loop proportional and integral control, forms the closed-loop predictive lift control to accomplish the exhaust valve lift tracking. The developed strategy is validated using an exhaust valve model based upon a 5.4L 3 valve V8 engine. It turns out that only 24 multiplications are need for each predictive step, which makes it feasible for real-time implementation.

References

[1] K. Inoue, K. Nagakiro, Y. Ajiki, and N. Kishi, "A High Power Wide Torque Range Efficient Engine with a Newly Developed Variable Valve Lift and Timing Mechanism," SAE 890675, 1989.

[2] Y. Moriya, A. Watanabe, U. Uda, H. Kawanura, M. Yoshioka, and Adachi, "A Newly Developed Intelligent Variable Valve Timing System Continuously Controlled Cam Phasing as Applied to a New 3 Liter Inline 6 Engine," SAE 960579, 1996.

[3] R. Flierl and M. Kluting, "The Third Generation of New Fully Variable Valvetrain for Throttle Free Load Control," SAE 2000-01-1227, 2000.

[4] M. Theobald, B. Lequesns, and R. Henry, "Control of Engine Load via Electromagnetic Valve Actuators," SAE 940816, 1994.

[5] C. Boie, H. Kemper, L. Kather, and G. Corde, "Method for Controlling a Electromagnetic Actuator for Achieving a Gas Exchange Valve On a Reciprocating Internal Combustion Engine," US Patent 6,340,008, 2000.

[6] L. Schneider, "Electromagnetic Valve Actuator with Mechanical End Position Clamp or Latch," US Patent 6,267,351, 2001.

[7] I. Haskara, L. Mianzo, and V. Kokotovic, "Method of Controlling an Electromagnetic Valve Actuator," US Patent 6,644,253, 2003.

[8] Y. Wang, A. Stefanopoulou, K. Peterson, T. Megli, M. Haghgooie, "Modeling and Control of Electromechanical Valve Actuator," SAE 2002-01-1106, 2002.

[9] G. Wright, N. Schecter, and M. Levin, "Integrated Hydraulic System for Electro-hydraulic Valvetrain and Hydraulically Assisted Turbocharger," US Patent 5,375,419, 1994.

[10] O. Sturman, Hydraulic Actuator for an Internal Combustion Engine," US Patent 5,638,781, 1994.

[11] Z. Sun and D. Cleary, "Dynamics and Control of an Electro-Hydraulic Fully Flexible Valve Actuation System," Proceedings of American Control Conference, Denver, Colorado, June, 2003.

[12] Jia Ma et al., "Analysis and Modeling of an Electronically Controlled Pneumatic Hydraulic Valve for an Automotive Engine," SAE 2006-01-0042, 2006.

[13] Jia Ma et al., "Model reference adaptive control of a pneumatic valve actuator for infinitely variable valve timing and lift," SAE 2007-01-1297, 2007.

[14] Jia Ma et al., "Adaptive control of a pneumatic valve actuator for an internal combustion engine," Proceedings of American Control Conference, New York, NY, July, 2007.

[15] M. Anderson, T. C. Tsao, M. Levin, "Adaptive Lift Control for a Camless Electro-hydraulic Valvetrain," SAE 981029, 1998.

[16] K. Misovec et al., "Digital Valve Technology Applied to the Control of a Hydraulic Valve Actuator," SAE 1999-01-0825, 1999.

[17] J. Ma, G. Zhu, T. Stuecken, A. Hartsig, and H. Schock, "Electro-pneumatic exhaust valve modeling and control for an internal combustion engine," Proceedings of ASME ICE Spring Conference, Chicago, IL, April, 2008.